RSC Advances




ROYAL SOCIETY OF CHEMISTRY

www.rsc.org/advances

# Synthesis, characterization, photophysical, thermal and electrical properties of composite of polyaniline with zinc bis(8-hydroxyquinolate): a potent composite for electronic and optoelectronic use.

**Ferooze Ahmad Rafiqi*, Kowsar Majid**

Department of Chemistry, National Institute of Technology, Hazratbal Srinagar, 190006, J&K, India.

*Corresponding author: Tel.: +91 9797237588; fax: +91 1942420475

Email-address:feroozerafiqi@rediffmail.com kowsarmajid@rediffmail.com

**Abstract**

Composite of polyaniline (PANI) with the metal complex of zinc bis(8-hydroxyquinolate) [$Zn(8HQ)_2$] is synthesized by In-situ polymerization technique. Metal complex and the synthesized PANI-[$Zn(8HQ)_2$] composite are characterized by EDX, FTIR, XRD and TG analysis. FESEM analysis display distinct morphological features of PANI and PANI-[$Zn(8HQ)_2$] composite. XRD shows crystalline nature of metal complex which was retained in the PANI-[$Zn(8HQ)_2$] composite. TG reveals higher thermal stability of PANI-[$Zn(8HQ)_2$] composite as compared to pure PANI. DSC exhibits increase in the glass transition temperature of PANI-[$Zn(8HQ)_2$] composite which indicated its rigid nature. UV-Visible spectral characterization confirms red shift of polyaniline upon doping with the zinc complex. Metal complex exhibits excellent photophysical property, good thermal stability and conducting behavior. The fluorescence intensity of PANI-[$Zn(8HQ)_2$] composite is found much higher than pure PANI. Relative fluorescence quantum yield of PANI-[$Zn(8HQ)_2$] composite is a few orders of magnitude higher than pure PANI. Conductivity of PANI-[$Zn(8HQ)_2$] composite is greater than pure PANI as detected by four probe method and IV

characteristics suggest semiconducting and conducting behavior of pure PANI and PANI-[$Zn(8HQ)_2$] composite, respectively. The aforementioned results suggest that the synthesized polymer composite is a potent material for electronic and opto-electronic applications such as light emitting diodes, solar cells and other semiconductor devices.

Keywords: polyaniline; zinc complex; thermal stability; fluorescence, conducting nature

## 1 Introduction

Since the accidental discovery of polyacetylene and the work on the related research area, by three noble laureates Macdiarmid, Heeger and Shirakawa, conjugated polymers have emerged as one of the thrust areas of scientific research [1-3]. Among all conjugated polymers, polyaniline is the most extensively studied polymer that has unique optical, electrical and chemical behavior [4-8]. Polyaniline has several advantages such as plasticity, environmental stability, protonating de-protonating tendency, affordiability, light weight and ease of fabrication [9], owing to which it finds applications in photovoltaic cells [10], organic light emitting diodes [11], sensors [12], adsorbents [13], electromagnetic shielding [14, 15], capacitors [16, 17], supercapacitors [18-20] and anticorrosive agents [21]. The negative aspects of polyaniline are low processcebility, poor thermal stability, weak luminescence and low conductivity as compared to metals etc. which limits its applications [22]. By adultering the PANI with foreign moieties, improvement in some of the properties can be achieved. Literature survey revealed a significant change in the chemical structure of polyaniline after doped with metals, metallic oxides, CNT's, inorganic ions etc.[9, 23,]. Emeraldine salt of polyanilne provides hole injecting electrodes in electroluminescent devices is one of the hot areas of research in the field of polymer optoelectronics. The conductivity in PANI has been increased to an unprecedented value, same almost in metals, after doping it with protonic acid HCl, that is why, sometimes it is called synthetic metal [22]. The doping in

conducting polymers with metal complexes has been a recent idea of chemists. In this connection, so many metal complex based composites of Polyaniline and polythiophene have been investigated by our group [24-27].

Macrocyclic metal complexes or chelated complexes have intrigued a lot of interest among material scientists worldwide because of their biological and chemical properties. The importance and stability of such metal complexes depends up on a number of factors, including the number and size of the chelate rings formed on complexation, stereochemistry of metal complex, number and type of the donor atoms present in the ligand and their relative positions within the macrocyclic skelton and also on the metal cation dimension. These complexes find wide range of applications in drug industry, cosmetics, metal catalysts, metalloenzymes etc. [28]. Macrocyclic ligands with $\pi$ - conjugation can improve the optical properties of metal complex. Zinc (II) is a suitable metal for any metal complex to show luminescence due to its $d^{10}$ electronic configuration because the excitation of electrons takes place easily [29]. 8-hydroxyquinoline is the best choice of ligand for any luminescent metal complex due to its electron transporting behavior. 8-hydroxyquinoline has potential biological activities, covers a wide range of applications which includes antioxidative abilities, diastolic functions, antibacterial actions, antivirus and antiplatelet activations and antitumurous effects [30]. Literature survey witnessed the synthesis of some luminescent Zn (II) complexes with N-heterocyclic ligands such as pyridine and imidiazole [31]. Here we report a Zn (II) complex with 8-hydroxyquinoline and investigate its doping tendency into polyaniline composite. 8-hydroxyquinoline is perhaps the unique ligand with not only having $\pi$ – conjugation but possesses heteroatoms of nitrogen and oxygen. These diverse coordination sites can produce interesting properties and overall functionality of the metal complex. 8-hydroxyquinoline metal chelates are considered the most reliable electron-transporting and emitting materials in molecular optoelectronics owing to their

high thermal stability, high fluorescence and excellent electron-transporting mobilities [32].

The present study involves the synthesis of PANI composite with $Zn(8HQ)_2$ and the role of dopant in improving photophysical, thermal and electrical properties of PANI composite. The dopant which we have opted is having high thermal stability and excellent photophysical property besides being conductive in nature. Owing to water insoluble character of $Zn(8HQ)_2$ and slight solubility in concentrated HCl, the synthesis of polyaniline composite has been carried out in aqueous medium. The synthesized materials have been subjected to thermal analysis and other spectroscopic characterization. In this paper, we report on the preparation of fluorescent as well as conducting composite of polyaniline with zinc bis(8-hydoxyquinolate) complex. The composite shows a noticeable fluorescence in the violet and blue region of the visible spectrum, with a relative quantum yield value a few orders of magnitude higher than to pure PANI. The electrical conductivity of composite has augmented to a significant value and is much higher than that of pure PANI. We also report that the thermal stability of composites improved upon doping with $Zn(8HQ)_2$ moieties and that is an advantage for optoelectronic device fabrication, because the use of such materials with high thermal stability can provide the device a greater longevity.

## 2 Experimental

### 2.1 Materials

Zinc Chloride (99.9%), 8-hydroyquinoline and concentrated HCl were of Merck quality. Aniline was supplied by Loba chemicals and used after distillation. Ammonium persulphate was also supplied by Loba chemicals. All the reagents and solvents used were of analytical grade. Triply distilled water was used for the synthesis.

### 2.2 Instrument and measurements

The FTIR spectra were recorded on a PerkinElmer spectrometer using KBr pellets. Elemental analysis for C, H and N was performed using a Vario EL elemental analyzer. Energy dispersive X-ray (EDX) of Bruker model was used for the investigation of elemental composition. XRD data was collected from PW-3050 base diffractometer with Cu $K_\alpha$ radiation of 1.540598 A°. Surface morphology of the samples was studied on Hitachi scanning electron microscope model S-3600N. Conductance measurement was carried out in DMSO solutions using a model Labindia Pico+ Conductivity Bridge. Ultraviolet-visible (UV-vis) spectra were taken on double beam UV-Visible spectrophotometer T 80. The fluorescence spectral analysis was conducted on an Agilent Technologies Cary Eclipse fluorescence spectrophotometer. The thermal analysis was carried out on a PerkinElmer thermal analyzer in $N_2$ atmosphere at a heating rate of 10 °C/min. DSC was carried out by Mettler Toledo DSC 822 e. The temperature range was from 30°C to 325°C at the heating rate of 10°C/min. The electrical conductivity of synthesized materials was measured by the standard Four Probe Technique at 25°C with Keithley mode 2400 (USA).

2.3 Synthesis of Zinc bis(8-hydroxyquinolate) [$Zn(8HQ)_2$]

1 mole of 8-hydroxyquinoline and 1 mole of NaOH are dissolved in 50 ml of $C_2H_5OH$. The whole solution is heated for 10 minutes at 50-60°C. On cooling, sodium 8-hydroyquinolate precipitates out. The precipitate obtained is dissolved in 50 ml of distilled water to prepare an aqueous solution. To this aqueous solution, 1 mole of $ZnCl_2$ is added. The solution is again heated for 10 minutes at 50-60°C. On cooling, yellow coloured zinc bis(8-hydroxyquinolate) precipitates out. The final product obtained after filtration is washed with $CH_3OH$ and dried in an oven at 50°C for 24 h. The dried sample is desiccated over fused $CaCl_2$ in a desiccator. The following reactions are assumed to occur in the ethanol and aqueous medium for the synthesis of $Zn(8HQ)_2$ .

$C_9H_7NO + NaOH \xrightarrow{C_2H_5OH} C_9H_6NONa\downarrow + H_2O$

$C_9H_6NONa + \text{aqueous medium} \rightarrow C_9H_6NO^- (aq.)$

$ZnCl_2 + 2C_9H_6NO^- (aq.) \xrightarrow{H_2O} Zn(C_9H_6NO)_2\downarrow + 2HCl$

2.4 Synthesis of PANI

2 ml of 10.6 M distilled aniline is dissolved in 10 ml of concentrated HCl solution. The mixture solution is cooled in a refrigerator for 10 minutes. Then the mixture solution is dissolved in 150 ml of distilled water. After that, 30 ml of aqueous solution containing 4.5 g of $(NH_4)_2S_2O_8$ is added dropwise over a period of 0.5 h in order to avoid heating the reaction mixture. The solution kept for magnetic stirring is allowed to continue at -5℃ for 6h. The final solution is filtered and greenish black precipitate obtained is washed with $CH_3OH$ and distilled water. Then it is dried in an oven at 40℃ for 24 h and the dried sample is put in a desiccator for desiccation.

2.5 Synthesis of PANI-$[Zn(8HQ)_2]$ composite

2 ml of 10.6 M distilled aniline and 10 ml of concentrated HCl is mixed and cooled in a refrigerator for 10 minutes. The mixture is then added to 150 ml of distilled water. 2.0 g of thermally synthesized $[Zn(8HQ)_2]$ is added to the whole mixture solution. For polymerization to commence, 30 ml of aqueous solution containing 4.5 g of $(NH_4)_2S_2O_8$ is added to the solution dropwise by constant stirring over a period of 0.5 h. The reaction mixture kept for magnetic stirring is allowed to proceed for 6h at -5℃. The greenish precipitate obtained after filtration is washed with $CH_3OH$ and then with distilled water. It is dried in an oven at 40℃ for 24 h and then, the dried sample is stored in a desiccator.

**3 Results**

3.1 Elemental Analysis and Energy dispersive X-rays (EDX)

The empirical formula assigned to the zinc (II) complex is $[Zn(C_9H_6NO)_2]$ 0.5 $H_2O$. Presence of water is also confirmed from thermogravimetric analysis (TG). The observed percentage of C, H and N are 60.44, 3.60 and 7.84 against calculated values of 60.33, 3.63 and 7.82, respectively. Energy dispersive X-rays (EDX) is used to analyze the elemental composition of $[Zn(8HQ)_2]$ and PANI-$[Zn(8HQ)_2]$ composite as shown in Fig. 2 a, b. EDX graph of PANI-$[Zn(8HQ)_2]$ composite is a direct evidence of incorporation of $[Zn(8HQ)_2]$ into the PANI matrix as it shows a prominent peak of Zn at 8.32 Kev. On the basis of elemental analysis, conductance measurements, FTIR and TG results, four-coordinated chelated structure has been proposed for the zinc (II) complex as shown in Fig. 1.

3.2 Conductance measurements

The molar conductance value of the zinc (II) complex in DMSO solution ($10^{-4}$ M) at 25°C is 18.21 $cm^2\ \Omega^{-1}\ mol^{-1}$, which is lower than the range reported for electrolytes in DMSO solutions [29].Such a low value of ionic conductance could be because of the chelated structure of the zinc (II) complex and the absence of any ionic moiety outside its coordination sphere. The chelated molecules on dissolution supply a very low number of ions in the solution, resulting in a very low value of overall ionic conductance. These results reveal the light electrolyte nature of the zinc (II) complex and indicate that the ligand 8-hydroxyquinolinate was successfully chelated with the zinc ion.

3.3 Fourier Transform Infrared (FTIR) Spectral characterization

The FTIR spectrum of $[Zn(8HQ)_2]$, pure PANI and PANI-$[Zn(8HQ)_2]$ composite are shown in Fig. 3 a-c. $[Zn(8HQ)_2]$ 0.5 $H_2O$ shows IR absorption peaks at 3510 $cm^{-1}$ due to O-H stretching of hydrated water, 1700 $cm^{-1}$ due to C=N stretching and 1523 $cm^{-1}$ is assigned for C=C symmetric stretching vibration of 8-hydroxyquinoline moiety [33]. Peak at 1250 $cm^{-1}$ is due to C— O stretching vibration and 1105 $cm^{-1}$ is attributed to C—

O—M stretching vibration [34]. The peaks observed at 840 $cm^{-1}$ and 710 $cm^{-1}$ are due to stretching vibrations of M—N and M—O bonds [35]. Peak at 850 $cm^{-1}$ shows the presence of 8-hydroxyquinoline which corresponds to the skeleton vibration of aromatic heterocyclic ring containing nitrogen [36]. Pure PANI shows a peak at 3251 $cm^{-1}$ for NH stretching. A peak at 1446 $cm^{-1}$ can be due to C—N + C—H bending mode of vibration. A peak at 1506 $cm^{-1}$ confirms the presence of a protonated imine group [37]. Peak at 1700 $cm^{-1}$ is due to C=NH stretching vibration and another peak at 900 $cm^{-1}$ can be ascribed to C—H out of plane bending. A peak at 2900 $cm^{-1}$ is assigned for C—H aromatic stretching. The FTIR of composite contains the absorption peaks at 3300 $cm^{-1}$ (N—H stretching), 2850 $cm^{-1}$ (C—H aromatic stretching), 1720 $cm^{-1}$ (υ C=N), 1536 $cm^{-1}$ (υ C=C), 1250 $cm^{-1}$, 900 $cm^{-1}$ (C—H out of plane bending), 850 $cm^{-1}$ (υ M—N),700 $cm^{-1}$ (υ M—O) and a peak at 750 $cm^{-1}$ confirms para-disubstituted aromatic rings indicating polymerization [38-41].A broad peak at 3514 $cm^{-1}$ shows the presence of lattice water, also confirmed from thermogravimetric analysis. The peaks observed in the FTIR of dopant appear in the composite with a shift of about $\pm 50-100$ $cm^{-1}$, suggesting an interfacial interaction between zinc (II) complex and PANI chains.

3.4 X-ray diffraction (XRD) characterization

X-ray diffraction (XRD) analysis were conducted on PW-3050 base diffractometer with Cu $K_\alpha$ radiations (scanning range 2θ: 15°-60°). Fig. 4 a-c, shows the XRD pattern of $[Zn(8HQ)_2]$, pure PANI and PANI-$[Zn(8HQ)_2]$ composite. XRD of $[Zn(8HQ)_2]$ shows sharp peaks at 2θ values of 25.1°, 30.3°, 32.0°, 33.7°, 38.1°, 46.1° and 58.6°. Polyaniline shows two broad diffraction peaks centered at 2θ values of 21.2° and 26.1°, which are the characteristic peaks of emeraldine salt of polyaniline [20, 42,]. These peaks appear in the composite at 2θ values of 20.5° and 25.7°. The peaks of $[Zn(8HQ)_2]$ appear in the composite at 2θ values of 24.4°, 31.1°, 32.9°, 39.8°, and 58.5°, respectively. Most of the

peaks have shown a shift of ∓0.5°, which suggests that polyaniline undergoes interfacial interaction with [Zn(8HQ)$_2$] crystallites and looses its own morphology by its deposition over [Zn(8HQ)$_2$] crystallites [43]. [Zn(8HQ)$_2$] is extremely crystalline in nature. Pure polyaniline is amorphous while the PANI-[Zn(8HQ)$_2$] composite is semi- crystalline in nature, revealing the impact of [Zn(8HQ)$_2$] on the polymer matrix.

Moreover, the average particle size of [Zn(8HQ)$_2$] and PANI-[Zn(8HQ)$_2$] composite was calculated using the Scherrer's equation (1):

$$L = {}^{K\lambda}/_{bCos\theta} \qquad (1)$$

Where λ = 1.540598 Å is the wavelength of Cu $K_\alpha$ radiation applied, θ is the Bragg angle ($^o$), b is the full width at half maximum of diffraction peak and K is the scherrer's constant (0.89). The average crystallite size of [Zn(8HQ)$_2$] and PANI-[Zn(8HQ)$_2$] composite comes out 156 nm and 172 nm. The increase of crystallite size may be attributed to the [Zn(8HQ)$_2$] particles which are deposited with PANI and amorphicity of PANI.

3.5 Field emission scanning electron microscope (FESEM) characterization

FESEM of pure PANI and PANI composite are shown in Fig. 5 a, b, respectively. FESEM figure of pure PANI shows spongy and porous structure, indicating its amorphous character. SEM figure of composite shows the globular structures arranged uniformly on the PANI matrix. These globular particles with average diameter varied from 0.5 to 2.0 $\mu$m, can be attributed to the [Zn(8HQ)$_2$] particles embedded in the PANI matrix. Some particles are big enough which may be due to the agglomeration of [Zn(8HQ)$_2$] particles or the coating of PANI over [Zn(8HQ)$_2$] particles. Comparative structural analysis of both the figures confirms the composite formation.

### 3.6 UV–Visible Spectra of PANI and PANI composite

UV-visible spectra of $Zn(8HQ)_2$, pure PANI and PANI composite are shown in Fig.6 a,b and c, respectively. $Zn(8HQ)_2$ shows two peaks, one at 315 nm and another at 415 nm. The first peak corresponds to $\pi-\pi^*$ electron transition of 8-hydroxyquinolate moieties and the second peak can be attributed to MLCT transition of metal to ligand $\pi^*$ orbital [30, 33, 35]. Pure PANI shows three absorption bands. One intense peak at 315 nm is assigned to the $\pi-\pi^*$ electron transition of the benzenoid segment. One more band at 480 nm is because of polaronic transitions (polaron band to $\pi^*$ band) and another band at 672 nm is due to the $\pi$ band to delocalized polaron band [5]. PANI composite shows peaks at 337 nm, 495 nm and 689 nm which can be ascribed to $\pi-\pi^*$ transition, polaron band to $\pi^*$ band and $\pi$ -polaron band transition of PANI, respectively. The presence of peaks above 600 nm indicates that the material is of emeraldine salt type and is conducting in nature [44]. The absorption bands are shifted towards longer wavelength as the dopant molecule was incorporated into PANI, indicating an interfacial attraction between dopant and polyaniline. The red shift of wavelength is attributed to increased conjugational length of PANI polymer.

### 3.7 Fluorescence characterization

Fluorescence emission spectra of $[Zn(8HQ)_2]$, pure PANI and PANI-$[Zn(8HQ)_2]$ composite are shown in Fig. 7 a-c and the luminescence data is presented in Table 1. $Zn(8HQ)_2$ in DMSO solution shows emission in radiative way at wavelength 432 nm when excited by different wavelengths; 342 nm, 360 nm and 382 nm. The results indicate that the zinc(II) complex emits in the violet region of electromagnetic spectrum. The fluorescence in metal complexes can be because of direct organic ligand excitation, MLCT or LMCT, d-d transition or ligand to metal energy transfer through antenna effect

[25]. 8-hydroxyquinoline can inject high electron density into the zinc component making it a fluorescent material. In [$Zn(8HQ)_2$] complex, 8-hydroxyquinoline can provide an efficient intra-molecular energy transfer from its triplet state to zinc ion as investigated in other transition and inner transition metal complexes [30, 31]. Therefore, 8-hydroxyquinoline can act as antenna in the zinc complex. It can be seen from the fluorescence spectrum of [$Zn(8HQ)_2$] that it possessed a very good fluorescence intensity.

Both pure PANI and PANI-[$Zn(8HQ)_2$] composite in NMP solution at 25°C shows excitation at wavelength 478 nm, when excited at 360 nm. These results indicate that both materials emit in the blue region of the electromagnetic spectrum. At the excitation wavelength of 340 nm, PANI-[$Zn(8HQ)_2$] composite shows an emission wavelength at 422 nm with high fluorescence intensity as shown in Figure 7 d. This result suggests that the composite can also emit in the violet region of the visible spectrum. However, the fluorescence intensity in pure PANI was too low as compared to its composite as the weak fluorescence of PANI is also reported in the literature [25]. Low fluorescence in pure PANI can be attributed to imbalance in the transportation rates of holes and electrons in the PANI chains [32]. In PANI-[$Zn(8HQ)_2$] composite, [$Zn(8HQ)_2$] complex can inject more and more electrons into the PANI chains via two ways. One way is the flow of electrons from the lone pair of oxygen into the polaronic and bipolaronic states of polyaniline. Another way is the transfer of electrons from the $d^{10}$ –filled electrons of zinc into the electron deficit regions of polyaniline. Hence electron transporting behavior of zinc (II) complex and hole transporting carriers of polyaniline chains is attributed to the increase of fluorescence in the PANI composite.

The relative fluorescence quantum yield of PANI-[$Zn(8HQ)_2$] composite ($\varphi_s$) is calculated against the pue PANI ($\varphi_r$ = 0.01 [45] ) taken as reference using excitation wavelength of 360 nm (Fig. (b) and Fig. (c)). For the determination of the relative

fluorescence quantum yield $\varphi_s$, we dissolve both pure PANI and PANI-Ni(acac)$_2$ composite in N-methyl 2-pyrollidone. The fluorescence quantum yield $\varphi_s$ is obtained by the use of standard Eq. (2) [45].

$$\varphi_s = \varphi_r \left[\frac{I_{(\lambda ref}}{I_{(\lambda s)}}\right] \left[\frac{\eta_{ref}^2}{\eta_s^2}\right] \left[\frac{A_{ref}}{A_s}\right] \left[\frac{D_s}{D_{ref}}\right] \qquad (2)$$

Where the subscripts 'ref' and's' refer the compound used as reference (PANI) and sample (PANI-[Zn(8HQ)$_2$] composite), respectively. I is the intensity of the fluorescence emission and η is the refractive index (η = 1.338 for both PANI and PANI-[Zn(8HQ)$_2$] composite in N-methyl 2-pyrollidone at 25°C). D is the measured integrated fluorescence intensity and A is the absorbance at the excitation wavelength (here, it is 360 nm). The $\varphi_s$ of PANI-[Zn(8HQ)$_2$] composite is calculated as 0.0997 from the Eq. (2).

Therefore percentage of quantum yield of PANI-[Zn(8HQ)$_2$] composite with respect to pure PANI = $\frac{0.0997}{0.01} \times 100 = 997$. Thus, fluorescence quantum yield of PANI-[Zn(8HQ)$_2$] composite ($\varphi_s$) is almost $10^3$ times more than that of PANI ($\varphi_r$).

3.8 Thermal Analysis

3.8.1 Thermogravimetric Analysis (TG Analysis)

The thermal analysis (TG–DTG) curves of dopant zinc complex, pure PANI and PANI composite are shown in Fig. 8 a-c and the thermoanalytical data is summarized in Table 2. Thermal analysis by TG–DTA technique determines the sequential and overall stability of the metal complex upon decomposition besides providing information about the composition of different moieties [27]. The TG decomposition curve of the zinc bis(8 hydroxyquinolate) hydrate complex shows the decomposition in two steps. The first decomposition which occurs in the temperature range of 80–160°C is related to the dehydration of lattice water. This step amounts to a weight loss of 2.55 % against the

calculated value of 2.51 %. The DTG temperature corresponding to this transition step is 128°C. The second transition occurs in the temperature range of 160–720°C with DTG maximum temperatures of 218°C.This step accounts for the 75.50 % weight loss against the calculated value of 75.98 %, which can be due to the loss of 8-hydroxyquinoline moiety. The thermal decomposition is incomplete even up to 720°C, due to the formation of thermally stable zinc oxide whose decomposition temperature is beyond the analysis range [45]. The residue remaining at 720°C is ZnO that amounts to 21.95 % of total weight against the calculated value of 21.51 %. The scheme of the water release along with other moieties from the complex is as follows:

$$[Zn(C_9H_6NO)_2]\ 0.5\ H_2O \xrightarrow{80^\circ C-160^\circ C} [Zn(C_9H_6NO)_2] +\ 0.5\ H_2O$$

$$[Zn(C_9H_6NO)_2] \xrightarrow{160^\circ C-720^\circ C} ZnO + C_{18}H_{12}N_2O$$

TG of pure PANI shows two transitions. One transition occurs in the temperature range of 110–220°C with a weight loss of 40.2% and is ascribed to the loss of water molecules embedded in the polymer matrix, HCl molecules and low molecular weight of polyaniline molecules. The DTG maximum temperature corresponding to this transition is 194.99°C. The second transition occurs in the temperature range of 220–720°C, corresponding to the degradation of polyaniline chain with DTG maximum temperature of 320.47°C. This steps amounts to 50% weight loss. About 91% of PANI decomposed at 720°C. PANI composite showing three transitions with the first one occurring in the temperature range of 65–133°C with maximum DTG temperature of 69.18°C and is attributed to the loss of lattice water molecules. This step accounts for 8.34% weight loss. The second transition occurs in the range of 135–241°C with a weight loss of 18% can be due to elimination of low molecular weight polyaniline. The DTG maximum temperature of this transition is 199.97°C. The third transition occurring in the temperature range of 241–720°C with DTG maximum of 328.80°C and can be attributed due to the

decomposition of polyaniline and breakdown of organic part of dopant. This step amounts to 38% weight loss. PANI composite gives a residue of 35.66% at 720℃ that may be due to ZnO and undecomposed PANI. Ti (Ti is the temperature at which the transition occurs) is the parameter that compares the thermal stability of molecules. Higher value of Ti indicates a higher thermal stability [22]. Setting aside the transition of lattice water loss, Ti for the decomposition of low molecular weight polyaniline in pure PANI is 110℃ and 135℃ in the case of the PANI composite. Ti values for degradation of polyaniline chains from pure PANI to PANI composites is 220℃ to 241℃. This 21℃ increase in Ti implies a higher thermal stability of the PANI composite than pure PANI.

Fig. 9 shows the thermogram of polyaniline composites with dopant concentrations of 20 %, 40 % and 45 %. The data of compositional analysis is shown in Table 3. The residue remaining at 720℃ of different polyaniline composites with 20 %, 40 % and 45 % dopant concentrations are 35.66 %, 52.93 % and 55.14 % of total mass, respectively. The results show that the thermal stability of the polyaniline composite increased upon doping with the zinc (II) complex. This could be because of the strong interfacial interactions between PANI and the zinc (II) complex. The zinc (II) complex, when engulfed in a large quantity in the PANI matrix, has a greater capability for restricting the polyaniline chains, thereby enhancing the thermal stability to an appreciable extent. Also, the Ti of PANI composites increase with the increase in dopant concentration, which further confirms the enhancement of thermal stability. At higher dopant concentration, thermal stability of PANI composite becomes even higher than the metal complex. This is due to the fact that during the thermal decomposition of polyaniline, more and more ZnO are formed, whose decomposition temperature is beyond the analysis range [46]. The rigidity of polyaniline chains further increases with the increase in dopant concentration due to extended interfacial interactions between dopant and PANI chains. The dopant may homogenize the distribution of molecular weight of PANI in the composite and hold it firmly by

means of interfacial interactions, thereby increases the thermal stability of PANI composite [47].

3.8.2 Differential Scanning Calorimetric Analysis

The differential scanning calorimetry (DSC) of the pure PANI and PANI composites is shown in Fig. 10. The DSC of pure PANI shows three endothermic transitions. The first transition, which occurs at a maximum temperature of 102℃, is attributed to the loss of lattice water. The second transition shows a broad endothermic dip at 124℃ which can be due to loss of HCl and low molecular weight polyanilne material. The third transition that occurs at maximum temperature of 180℃ represents the glass transition temperature ($T_g$) of polyaniline matrix. The DSC of the PANI composite shows three prominent endothermic transitions, one of which is very intense. First transition occurs at 103℃ is attributed to the loss of water of crystallization that might have embedded in the outer layers of polyaniline or hydrated water of metal complex. Second transition occurring at 145℃, can be due to loss of low molecular weight PANI. Third transition that occurs at 272℃ represents the glass transition temperature of polyaniline, including the decomposition of organic part of zinc (II) complex. The increase in $T_g$ from pure PANI to PANI-[$Zn(8HQ)_2$] composite can be due to the strong interfacial interaction between $Zn(8HQ)_2$ and polyaniline chains. A higher $T_g$ value of PANI-[$Zn(8HQ)_2$] composite is an advantage for optoelectronic device fabrication, because the use of fluorescent materials with high transition temperatures may provide the device with greater longevity [48].

3.9 Electrical conductivity

The conductivity values of [$Zn(8HQ)_2$], pure PANI and PANI-[$Zn(8HQ)_2$] composite as detected by the four-probe method are 12 S/cm, $1.4 \times 10^{-3}$ S/cm and 22 S/cm. The conductivity values demonstrated that [$Zn(8HQ)_2$] and PANI-[$Zn(8HQ)_2$] composite are

conductors and pure PANI a semiconductor. In the PANI-[$Zn(8HQ)_2$] composite, PANI and [$Zn(8HQ)_2$] crystallites due to strong interfacial interactions between them, as suggested by FTIR and XRD studies, changes the molecular conformation of PANI from compact coil like structure to an expanded coil like structure. As a result, there may be an augmentation in the conductivity of PANI-[$Zn(8HQ)_2$] composite. The opening up of coils tends to promote linear conformation necessary for crystallization. Increasing the crystallinity of polymer can increase the bulk conductivity as it is reported in the literature that the conductivity of conjugated polymers depends on their morphology, type of monomer, extent of conjugation, doping level and degree of crystallinity [26]. If the conductive filler is used, the conductivity of composites can be improved. Here [$Zn(8HQ)_2$] is conductive in nature, then the conductivity in PANI-[$Zn(8HQ)_2$] composite is definitely because of its presence in the PANI matrix. The [$Zn(8HQ)_2$] may serve as conducting bridges connecting the isolated polyaniline chains.

I-V characteristics

In case of PANI, at low voltages the current increases very slowly upto knee voltage, Fig. 11a, thereafter current shows an abrupt increase with a slight increase in voltage. The similar behavior is found in case of semiconductors. In composite Fig. 11 b, the current increases linearly with increase in voltage, showing ohmic behavior, characteristics of conductors. The augmentation in the conductance of PANI-[$Zn(8HQ)_2$] composite can be explained on the basis of generation of some additional energy levels associated with zinc (II) complex in between HOMO-LUMO energy gap, thereby decreasing band gap and increase in the number of charge defects. This fact is also supported by UV-Vis spectra of PANI and PANI composite. The high conductance of PANI-[$Zn(8HQ)_2$] composite can also be attributed because of the metallic nature of zinc metal, conjugation of $\pi$-electrons of quinoline ring with the $\pi$ −electrons of phenylene rings of PANI and transfer of lone

pair of electons from oxygen of metal complex to cationic and dicationic states of polyaniline.

## 4 Conclusion

Composite of PANI with this zinc (II) complex was obtained via chemical oxidative polymerization. EDX, UV–visible, FTIR, SEM, and XRD proved the successful synthesis of composite formation. Crystallite size of $[Zn(8HQ)_2]$, and PANI-$[Zn(8HQ)_2]$ was calculated by Scherrer's formula. Peak broadening in composite was essentially attributed to amorphicity due to PANI. Zinc (II) complex exhibits excellent photophysical property and inherits this property into polymer matrix successfully. The relative fluorescence quantum yield of PANI-$[Zn(8HQ)_2]$ composite is higher than pure PANI. Therefore, the synthesized materials can illuminate the applications in the fields of organic light emitting diodes (OLEDs). From TG and DSC, increase in thermal stability and rigidity of composite was observed. The increase of conductivity in the PANI-$[Zn(8HQ)_2]$ composite had been attributed to the increase in crystallinity of PANI due to uncoiling of PANI chains caused due to strong interfacial interactions with $[Zn(8HQ)_2]$ crystallites. The increase of conductivity can explore applications of polymer composites in the field of electronics and organic opto-electronics.

**Acknowledgments**

We wish to express our gratitude to the reseach institutions of SAIF STIC Kochi, NIT, Hamirpore and the Central Instrumentation facility, Jammia Millia Islamia, New Delhi, for providing the instrumentation facilities. The authors are also thankful to Prof. Rajat Gupta, Director of NIT Srinagar and S.A. Shah, Head of the Department of Chemistry, NIT, for their support and cooperation.

## References

[1] S. Yuan, R. Jaramillo, T. F. Rosenbaum and L. Yu, Macromolecules, 2006, **39**, 8652.

[2] M. A. El-Sherif, J. Yuan and A. G. MacDiarmid, J. Intelligent Mater. Sys. Struct., 2000, **11**, 407.

[3] X. Hongyao, W. K. Shiao, S. L. Juh and C. C. Feng., Macromolecules, 2002, **35**, 8788.

[4] A. G. MacDiarmid, Synth. Met. 2002, **125**, 11.

[5] B. K. Kuila and M. Stamm, J. Mater. Chem., 2010, 20, 6086.

[6] S. Kant, S. Kalia and A. Kumar, J. alloys compd., 2013, 578, 249.

[7] R. R. Urkude, P. T. Patil, S. B. Kondawar and U. A. Palikundwar, Procedia Materials Science, 2015, 10, 205.

[8] A. A. Ragachev, M. A. Yarmolenko, J. Xiaohong, R. Shen and P. A. Lucknov, Applied Surface Science, 2015, 351, 811.

[9] S. W. Phang, M. Tadokoro, J. Watanabe and N. Kuramoto, Current Applied Physics, 2008, **8**, 391.

[10] B. Massoumi, V. Badr-Valized and M. Jaymand, RSC Adv., 2015, 5, 40840.

[11] A. Shahalizad, S. Ahamadi-Kandjani, H. Movla, H. Omidi, B. Massoumi, M. S. Zakerhamidi and A. A. Entezami, Opt. Mater., 2014, 37, 760.

[12] K. Majid, S. Awasthi and M.L. Singla, Sensor Actuat. A-Phys., 2007, **135**, 893.

[13] M. Bhaumik, A. Maity, V. V. Srinavasu and M. S. Onyango, Journal of Hazardous Materials, 2011, **190**, 381.

[14] H. R. Tantawy, D. E. Aston, J.R. Smith and J. L. Young, ACS, Appl. Mater. Interfaces, 2013, 5, 4648.

[15] W. Wang, S. P. Gunfekar, Q. Jiao and B. Zhao, J. Mater. Chem. C, 2013, 1, 2851.

[16] M. N. Nadagouda and R. S. Varma, Green, Chem., 2007, 9, 632.

[17] P. Prabunathan, K. Sethuraman and M. Alagir, RSC Adv., 2014, 4, 47726.

[18] C-G. Wu, H-T. Hsiao and Y-R. Yeh, J. Mater. Chem., 2001, 11, 2287.

[19] X. Wang, D. Liu, J. Deng,X. Duan, J. Guo and P. Liu, RSC. Adv., 2015, 5, 78545.

[20] S. W. Phang, M. Tadokoro, J. Watanabe and N. Kuramoto, Synth. Met., 2008, **158**, 251.

[21] A. Olad, M. Barati and H. Shirmohammadi, Progress in organic Coatings, 2011, 72, 599.

[22] M. S. Rather, K. Majid, R. K. Wanchoo and M. L. Singla, Synth. Met., 2013, **179**, 66.

[23] T. Bashir, A. Shakoor, E. Ahmad, M. Saeed, N. A. Niaz and S. K. Tirmizi, Polymer Science, Ser. B., 2015, **57** (3), 257.

[24] R. Rasool and K. Majid, Bull. Mater. Sci., 2014, **37**(5), 1181.

[25] F. A. Rafiqi, K. Majid, Synth. Met., 2015, **202**, 147.

[26] F. A. Rafiqi and K. Majid, Journal of Environmental Chemical Engineering, 2015, **3**, 2492.

[27] F. A. Rafiqi and K. Majid, Chem. Pap., 2015, **69** (10), 1331.

[28] F. Patrascu, M. Badea, M. N. Grecu, et al. J. Therm. Anal. Calorim., 2013, **113**, 1421.

[29] C. Zhong, Y. He, H. Zhou, L. Xiao, Y. Liu and H. Zhang, Materials Letters, 2009, **63**, 1413.

[30] J. Xie, L. Fan, J. Su and H. Tian, Dyes and Pigm., 2003, **59**, 153.

[31] Y-W. Li, Y. Tao and T-L. Hu, Solid State Sciences, 2012, **14(8)**, 1117.

[32] H-P. Zeng, G-R. Wang, G-C. Zeng and J. Li. Dyes and Pigm., 2009, **83**, 155.

[33] L. Feng, X. Wang, S. Zhao and Z. Chen, Spectrochimica Acta Part A., 2007, **68**, 646.

[34] F. Rizzo, F. Meinardi, R. Tubino, R. Pagliarin, G. Dellepiane and A. papagni, Synth. Met., 2009, **159**, 356.

[35] H. Huang, C. Zhong and Y. Zhou, Eur. Polym. J., 2008, **44**, 2944.

[36] C. Zhong, H. Huang, A. He and H. Zhang, Dyes and Pigm., 2008, **77**, 578.

[37] Y. Xia, T. Li, J. Chen and C. Cai, Synth. Met., 2013 **175**, 163.

[38] S.M. Reda and S.M. Al-Ghanan, Adv. Mater. Phys. Chem., 2012, **2**, 75.

[39] H. C. Pant, M. K. Patra, S. C. Negi, A. Bhatia, S. R. Vadera and N. Kumar, Bull. Mater. Sci., 2006, **29** (4), 379.

[40] J. Chen, J. Yang, X. Yan and Q. Xue, Synth. Met., 2010, **160** (23–24), 2452.

[41] T. Machappa, M.V.N.A. Prasad, Bull. Mater. Sci., 2012, **35** (1), 75.

[42] V. Eskizeybek, H. Gulce, A. Gulce and E. Akgul, J. Fac. Eng. Arch. Selcuk. Univ., 2012, **27**(4), 111.

[43] T. Mathavan, J. Archana, Y. Hayakawa, A. Anitha, M. A. Jothirajan, A. Divya, A. M. F. Benial, International Journal of ChemTech Research, 2014-2015, **7**(3), 1253.

[44] J. Y. Shimano and A. G. MacDiarmid, Synth. Met., 2001, **123**, 251.

[45] K.G.B. Alves, E.F.D. Melo, C.A.S. Andrade and C.P.D. Melo, J. Nanopart. Res., 2013, **15**, 1339.

[46] C. Bucer, M. Badea, M. C. Chifiriuc. et al., J. Therm. Anal. Calorim., 2014, **115**, 2179.

[47] Z. Huang, S. Wang, H. Li, S. Zhang and Z. Tan, J. Therm. Anal. Calorim., 2014, **115**, 259.

[48] A.A. Soliman, M.A. Amin, A.E. Al-Sharief, S. Ozdemir, C. Varlikli and C. Zafer, Dyes and Pigm., 2013, **99**, 1056.

Tables

Table 1 The luminescence data of $Zn(8HQ)_2$, PANI and PANI-$Zn(8HQ)_2$ composite.

| Materials | $\lambda_{max.}$(nm) | $\lambda_{exc.}$(nm) | $\lambda_{emiss.}$(nm) |
|---|---|---|---|
| $Zn(8HQ)_2$ | 315, 415 | 342, 360, 382 | 432 |
| PANI | 315, 480, 672 | 360 | 478 |
| PANI-$Zn(8HQ)_2$ composite | 337, 495, 689 | 360 | 478 |
| | | 340 | 423 |

Table 2 Thermoanalytical data for the decomposition of $Zn(8HQ)_2$, PANI and PANI-$Zn(8HQ)_2$ composite.

| Materials | Temperature range (°C) | DTG (°C) | Weight Loss (%) | Remarks Removal of | Residue at 720°C |
|---|---|---|---|---|---|
| $Zn(8HQ)_2$ | 80-160 | 128 | 2.55 | Lattice water | 21.95% |
| | 160-720 | 218 | 75.50 | 8-hydroxyquinolate | |
| PANI | 110-220 | 194.99 | 40.20 | Lattice water, HCl, Low Mol. Wt. PANI | 9.80% |
| | 220-720 | 320.47 | 50.00 | Breakdown of PANI | |
| PANI-$Zn(8HQ)_2$ composite | 65-133 | 69.18 | 8.34 | Lattice water | 35.66% |
| | 135-241 | 199.97 | 18.00 | HCl, Low Mol. Wt. PANI | |
| | 241-720 | 328.80 | 38.00 | Breakdown of PANI, 8-hydroxyquinoline | |

Table 3 Compositional Analysis of $Zn(8HQ)_2$/PANI Composite.

| Materials | Amount of $Zn(8HQ)_2$ (%) | PANI (%) | $T_i$ (°C) | Residue at 720°C |
|---|---|---|---|---|
| Pure PANI | 0.0 | 100 | 220 | 9.80 % |
| PANI-$Zn(8HQ)_2$ composite | 20<br>40<br>45 | 80<br>60<br>55 | 241<br>292<br>310 | 35.66 %<br>52.93 %<br>55.14 % |

22

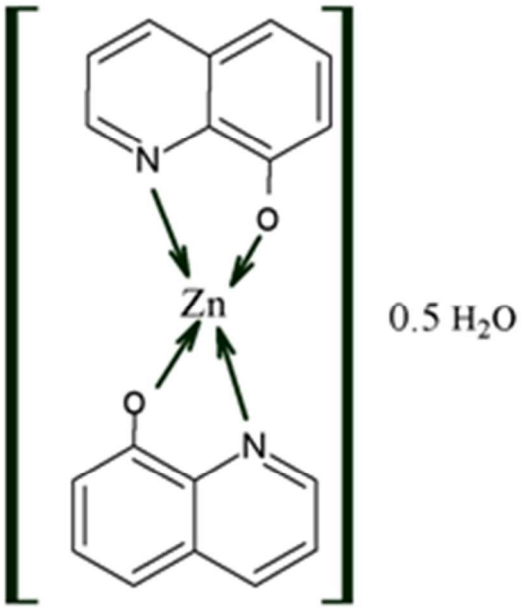


**Fig. 1** Structure of $[Zn(8HQ)_2]$

23

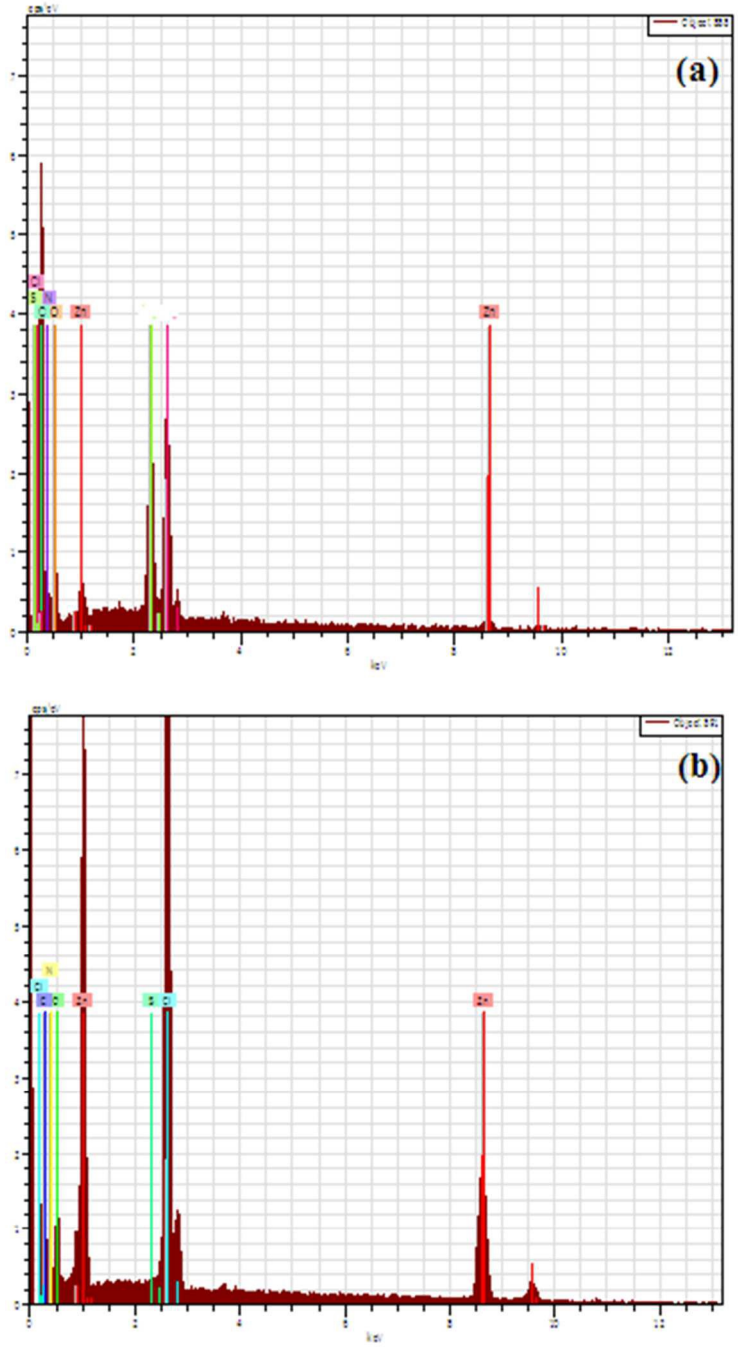


**Fig. 2** EDX of $[Zn(8HQ)_2]$ (a), and PANI-$[Zn(8HQ)_2]$ composite (b)

24

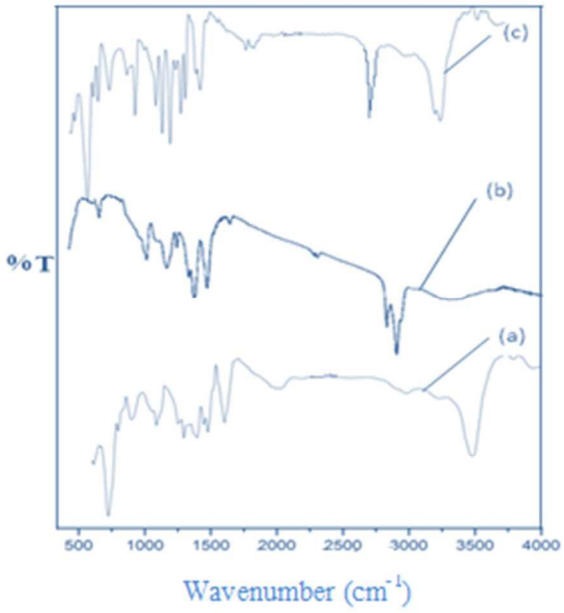


**Fig 3.** FTIR of $[Zn(8HQ)_2]$ (a), PANI (b), and PANI-$[Zn(8HQ)_2]$ composite (c)

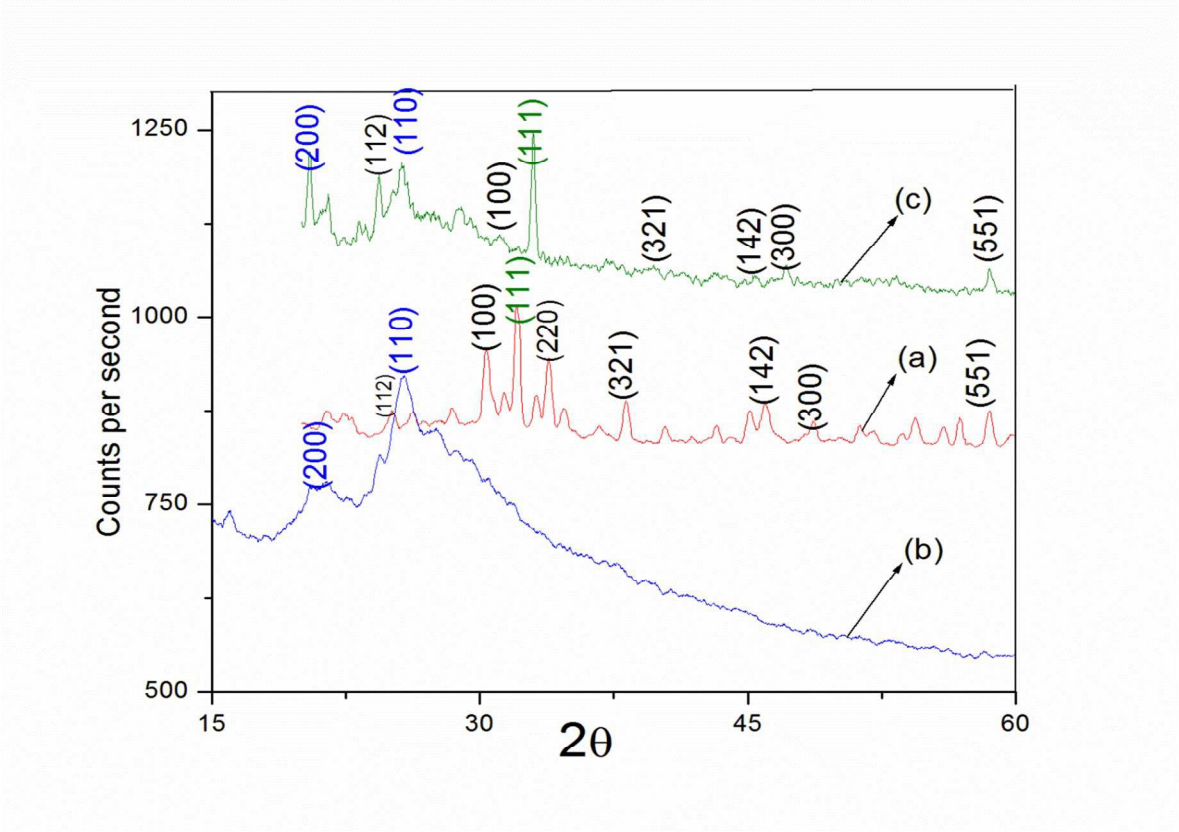


**Fig. 4** XRD of $[Zn(8HQ)_2]$ (a), PANI (b), and PANI-$[Zn(8HQ)_2]$ composite (c)

25

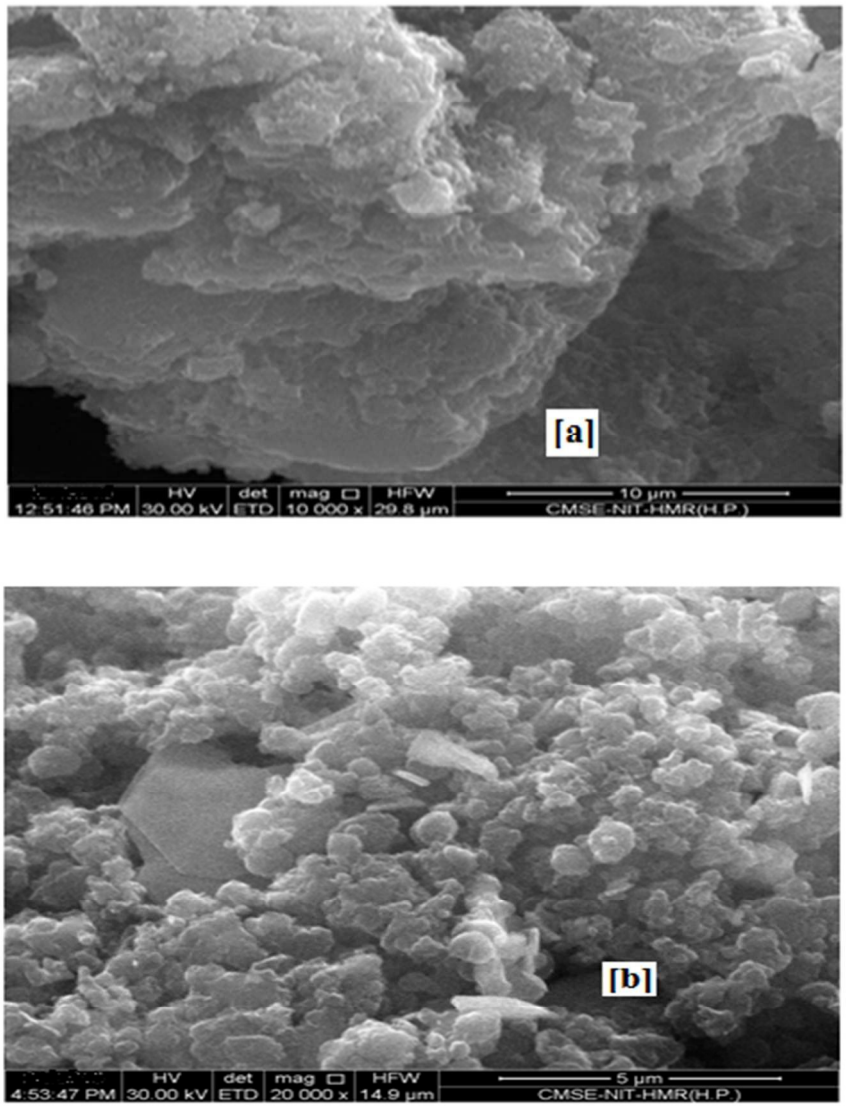


Fig. 5 FESEM of PANI (a), and PANI-[$Zn(8HQ)_2$] composite (b) .

26

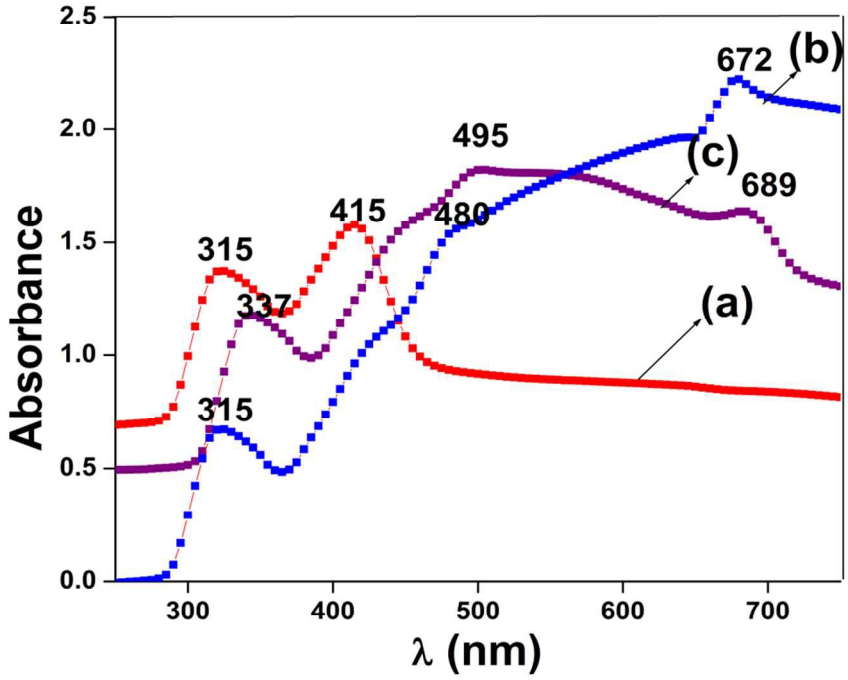


**Fig 6.** UV-visible spectra of $[Zn(8HQ)_2]$ (a), PANI (b), and PANI-$[Zn(8HQ)_2]$ composite (c).

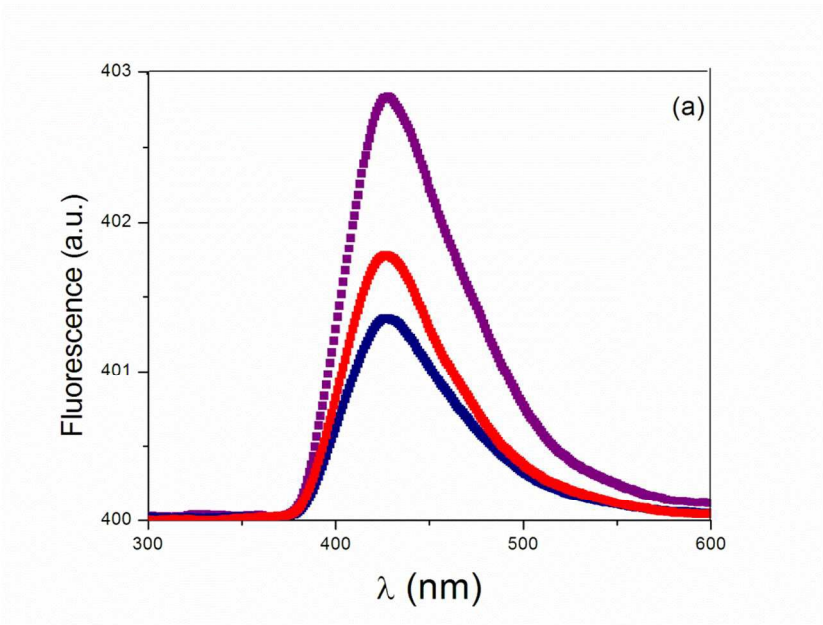

27

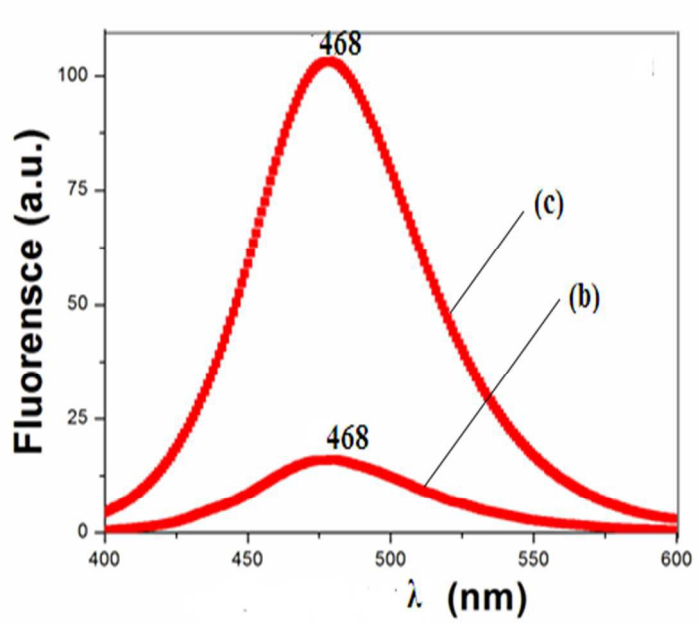


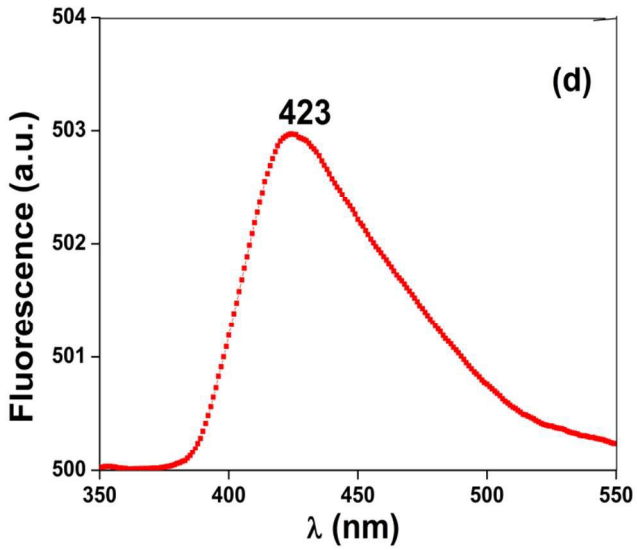


**Fig. 7** Fluorescence emission spectra of of $[Zn(8HQ)_2]$ (a), PANI (b), PANI-$[Zn(8HQ)_2]$ composite (c), when excited at 360 nm, and PANI-$[Zn(8HQ)_2]$ composite (d),when excited at 340 nm.

28

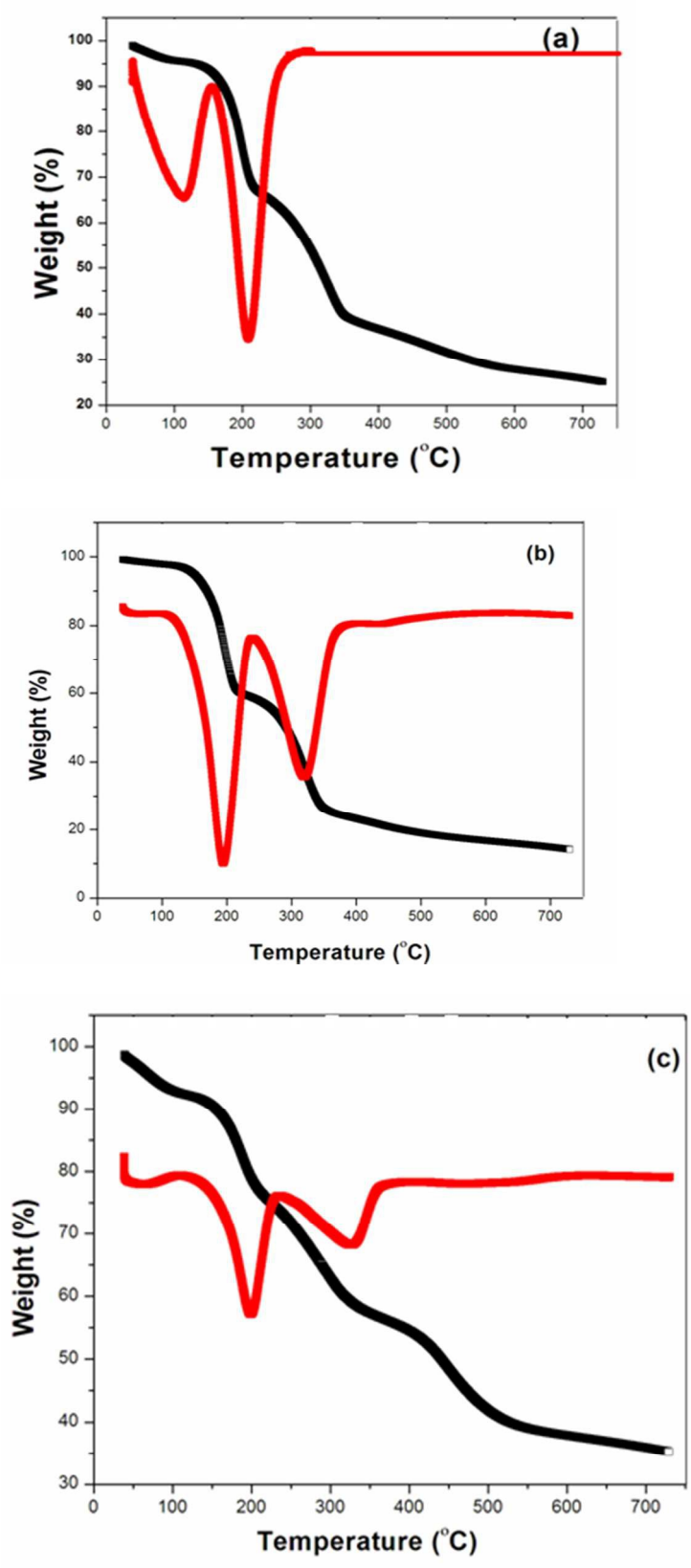


Fig. 8 TG graphs of of $[Zn(8HQ)_2]$ (a), PANI (b), and PANI-$[Zn(8HQ)_2]$ composite (c)

29

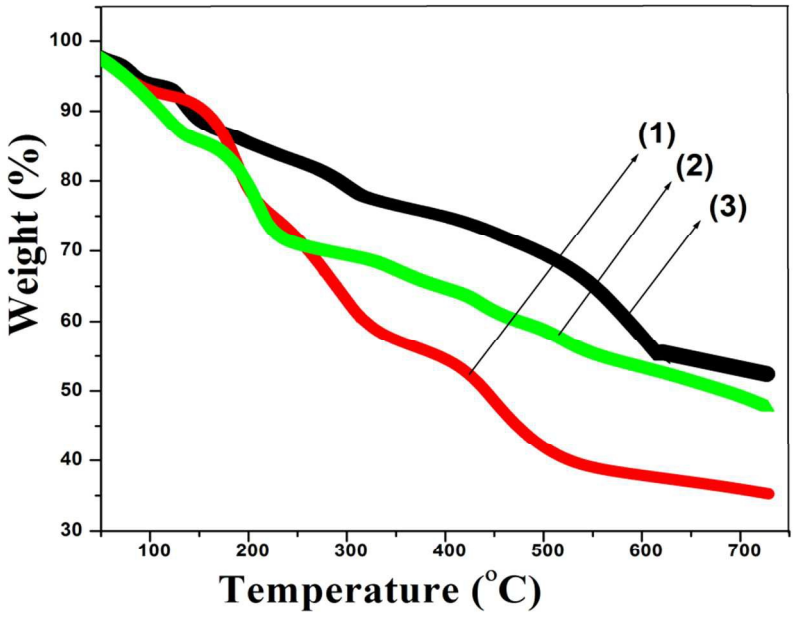


**Fig. 9** TG curves of PANI composite with different dopant concentration 20% (1), 40% (2), and 45% (3).

30

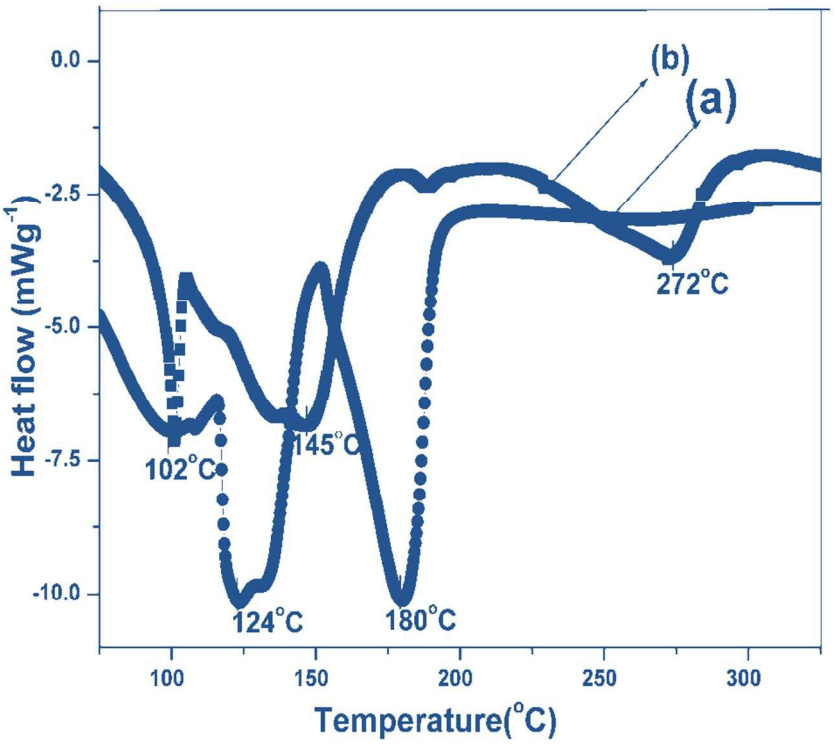


**Fig. 10** DSC of PANI (a), and PANI-[$Zn(8HQ)_2$] composite (b).

31

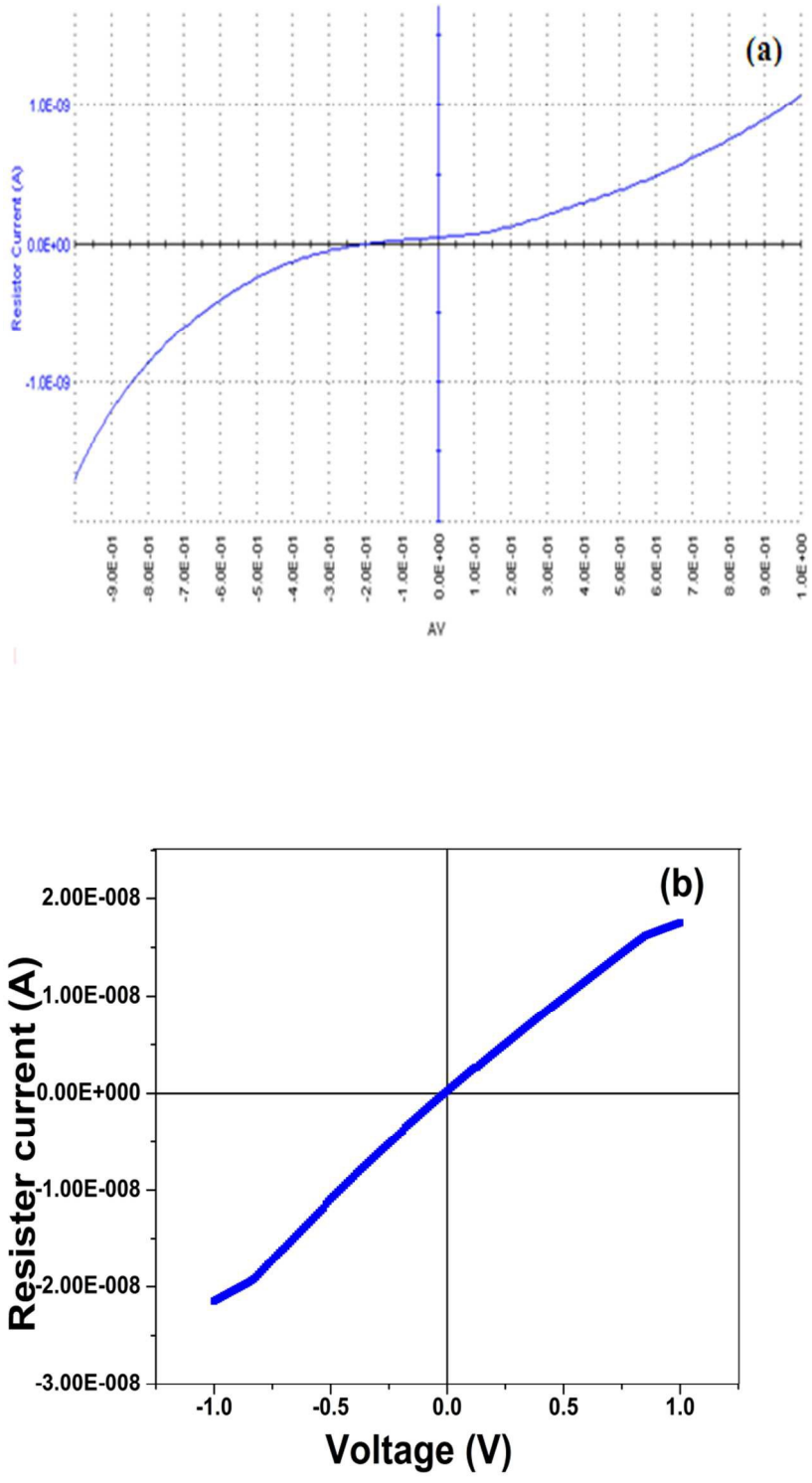


**Fig. 11** I-V curve of PANI (a), and PANI-[$Zn(8HQ)_2$] composite (b).

**A table of contents entry**

A novel fluorescent as well as conducting composite of polyaniline with zinc bis(8-hydroxyquinolate) complex, prepared via In-situ oxidative polymerization method.

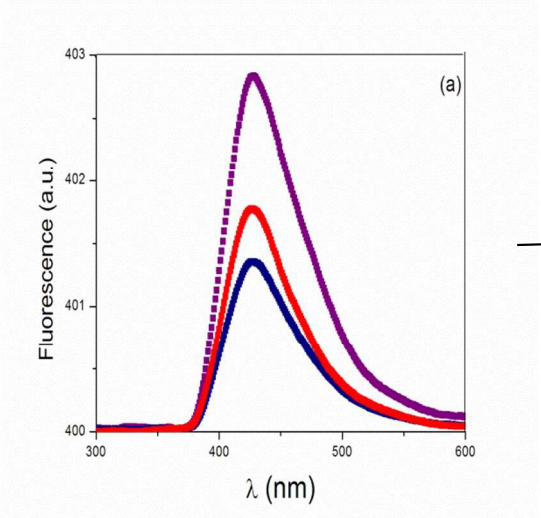


**Fluorescence of zinc complex (dopant)**

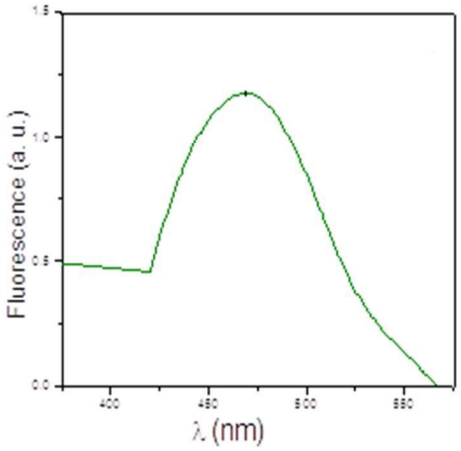


**Weak Fluorescence shown by pure PANI**

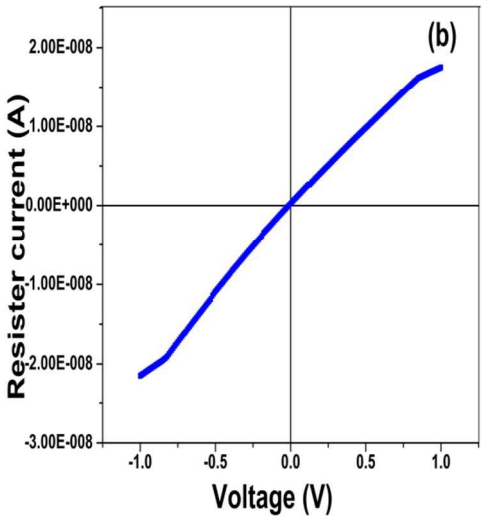


**Conducting behaviour of PANI composite**

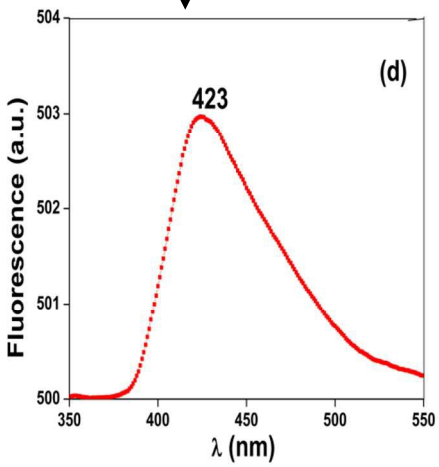


**Fluorescence of PANI Composite**